J. Fluid Mech. (1975), *vol.* 72, *part* 3, *pp.* 559–586
Printed in Great Britain

Free shear layer instability due to probes in rotating source–sink flows

By CARMEN P. CERASOLI

Geophysical Fluid Dynamics Program, Rutgers University,
New Brunswick, New Jersey 08903†

(Received 10 February 1975)

Experiments with a rotating source–sink annulus have shown that hot-wire probe supports can give rise to low-wavenumber, azimuthally propagating disturbances. These have been observed by a number of workers, and interpreted as Ekman boundary-layer instabilities and inertial eigenmodes of the annulus. The waves are associated with the wake downstream from the probe support; and a simplified model of the wake instability in cylindrical coordinates is presented. This model has a number of features in common with the observed disturbances. Extensive data have been obtained on wave frequencies and magnitudes, wavenumbers and phase relationships, and on wake structure and onset of the disturbances. The results of hot-wire anemometry experiments in an annulus are discussed in light of the present findings. It is concluded that the wave motions interpreted as type-II (class-A) Ekman instabilities and inertial eigenmodes by Tatro & Mollo-Christensen (1967) were probe-associated disturbances, while the boundary-layer waves observed by Caldwell & Van Atta (1970) were type-II disturbances, similar to those observed by Faller & Kaylor (1966*a*) using dye techniques.

1. Introduction

The rotating source–sink annulus has been used to study a number of flow problems; one area of research has been investigation of the stability of a laminar Ekman boundary layer. Unstable modes of the Ekman layer were first observed by Faller (1963) and Faller & Kaylor (1966*a*) using a water-filled annulus with dye techniques, and it was found that two types of instability could occur. The type-II (class-A) instability occurs at a Reynolds number ($Re = V\delta/\nu$, where V is the mean velocity, δ the Ekman depth and ν kinematic viscosity) of approximately 50, with wavelengths of order 25δ and phase speeds of order $\frac{1}{2}V$. The type-I (class-B) waves occur at $Re \simeq 125$, with wavelengths of order 10δ, and are either stationary or slowly moving.

The theoretical problem of Ekman-layer stability has been studied by Barcilon (1965), Lilly (1966) and Faller & Kaylor (1966*b*). Lilly used linear perturbation analysis and solved numerically the resulting eigenvalue problem;

† Present address: Geophysical Fluid Dynamics Program, Princeton University, P.O. Box 308, Princeton, N.J. 08540.

Faller & Kaylor (1966*b*) integrated numerically the nonlinear time-dependent equations. Both Lilly and Faller & Kaylor (1966*b*) found two types of instabilities with properties similar to the disturbances observed in the experiments of Faller (1963) and Faller & Kaylor (1966*a*). From the theoretical work, it was found that the type-I instability was associated with the inflexion point in the Ekman spiral, and was an inviscid instability. The mechanism for the type-II waves was realized by Lilly to be one where kinetic energy was released from an ordinarily stable velocity configuration, linear shear, by an ordinarily stabilizing influence, rotation. Such a mechanism was anticipated by Burgers (1953), who introduced energy conserving terms, analogous to the Coriolis force, into a set of equations modelling turbulent shear flow.

Tatro & Mollo-Christensen (1967) reported observing both classes of instability in a rotating source–sink annulus with air as the working medium and instrumented with hot-wire probes. They also reported observing interior wave motions, and interpreted these as inertial modes of the annulus excited by Ekman-layer instabilities. The investigation of these interior wave motions was continued by Green (1968), Green & Mollo-Christensen (1970) and Ingram (1971), who gave the same interpretation as Tatro & Mollo-Christensen. Caldwell & Van Atta (1970) also used a rotating source–sink annulus with air and hot-wire anemometry, and observed disturbances with properties similar to those predicted for the type-II instability.

The present work is the outcome of an attempt to study the generation of inertial waves by Ekman-layer instabilities. It was found that the disturbing effects produced by hot-wire probe supports (rods typically 2–3 mm diameter) were substantial. Azimuthally travelling disturbances can occur owing to the presence of a disturbing rod (or probe support); and the properties of these are similar to the reported properties of the interior waves observed by Tatro & Mollo-Christensen, Green and Ingram. The disturbances are associated with the wake produced by the rod or probe support, and have frequencies of order the rotation frequency. The waves are not a local phenomena and can typically be detected throughout the annulus. The disturbances have integer azimuthal wavenumbers m, which range from about 2 to 7, depending on the radial position of the disturbing rod r_R. Low values of m are associated with small r_R and high values of m with large r_R. These disturbances are very similar to the wave motions of detached shear layers studied by Hide & Titman (1967). The rod-induced waves also have properties similar to those reported for the disturbance labelled type-II instability by Tatro & Mollo-Christensen and Tatro (1966).

Disturbance effects due to probes have also been observed by Fultz & Kaiser (1971), in experiments using a differentially-heated, rotating annulus. Oscillations associated with the probe were observed, but not dealt with in detail, as their work concentrated on the effect of the probes on mean velocities. The oscillations did appear to have low wavenumbers in the interior and frequencies of the order of the rotation frequency (Fultz, personal communication).

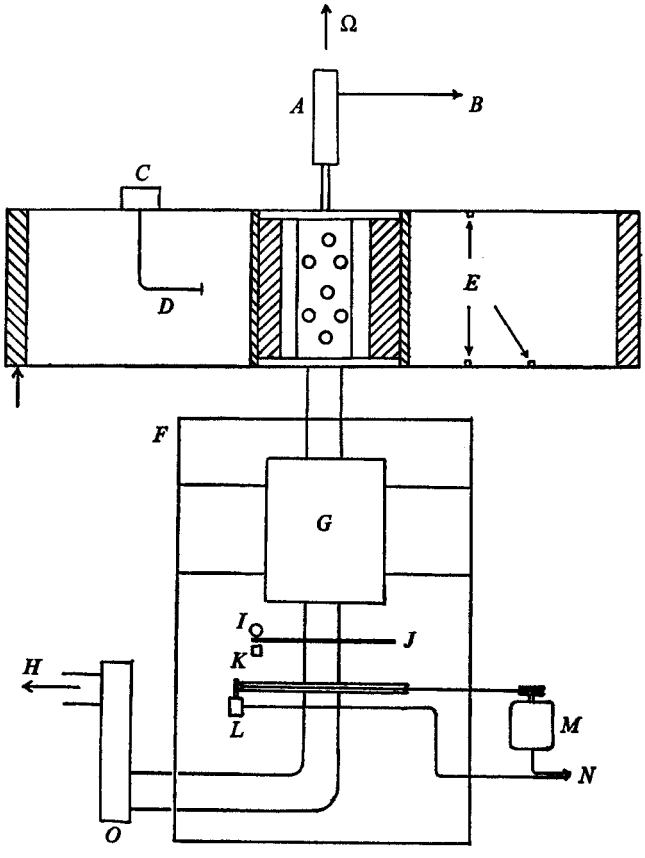

FIGURE 1. Schematic of apparatus used in source–sink annulus experiment. *A* Twelve mercury slip rings. *B* To Disa units. *C* Traverser. *D* Gooseneck support. *E* Non-disturbing probes. *F* Reticulated polyurethane foam. *G* Bearing support. *H* To baffle and vacuum system. *I* Light. *J* Perforated disk. *K* Photo-diode. *L* Tachometer. *M* D.c. motor. *N* To speed control. *O*, Flowmeter.

2. Experimental apparatus and techniques

The apparatus employed in this experiment is pictured in figure 1; it is similar in many respects to that designed by Green (1968). Polished aluminium plates 60·96 cm in diameter were separated by 10·48 cm by a central hub, which was perforated and covered with polyurethane foam; the radius of the inner wall was 11·48 cm. The outer wall was also polyurethane foam, which was very effective in spinning up the incoming air. A variable speed d.c. motor rotated the annulus via a belt drive and rotation speed was monitored with a tachometer and with a perforated disk, light source, photodiode and electronic counter. A vacuum pump was used to draw air through the annulus; and a stagnation chamber isolated the annulus from upstream disturbances. The volumetric flow rates were measured using a rotameter flowmeter with an accuracy of typically $\pm 5\%$.

The annulus was carefully aligned to minimize effects associated with misalignment; and the following specifications were obtained. The upper and lower

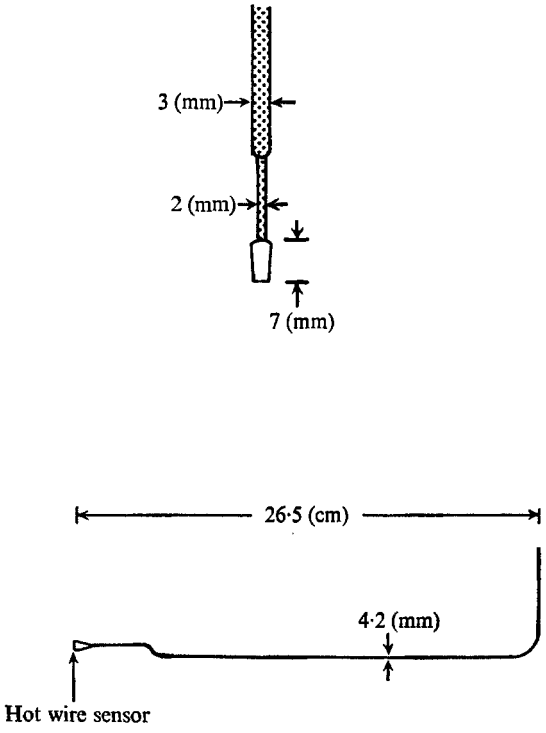

FIGURE 2. Hot-wire probe supports used in the experiments. The extended support allowed the sensor to be traversed to all radial positions.

plates were normal to the rotation axis to within 10^{-3} rad; and the rotation axis was within 10^{-3} rad of the vertical. The outer edges of the plates were concentric with the rotation axis to within 0·1 mm; and the plates were parallel to within 0·6 mm, with the departure from flatness due to warping from machining.

Access holes for hot-wire probes were placed at the following non-dimensional radii (outer radius = 1·000) and azimuthal positions: on the upper plate, $\phi = 0°$, $r = 0{\cdot}333$, $0{\cdot}500$; $\phi = 60°$, $r = 0{\cdot}333$, $0{\cdot}500$, $0{\cdot}667$, $0{\cdot}833$; $r = 0{\cdot}333$, $\phi = 180°$, $240°$; on the lower plate, $r = 0{\cdot}278$, $\phi = 50°$; $r = 0{\cdot}333$, $\phi = 60°$. An access hole at $r = 0{\cdot}580$, $\phi = 150°$ could be used for an extended probe support capable of sweeping a velocity sensor to all radii. Disa hot-wire anemometry was used; figure 2 shows the typical construction of a hot-wire probe and support, along with a picture of the extended probe support. The prongs holding the sensing wire are about 7 mm long and 0·5 mm in diameter, while the body of the probe support is about 3 mm in diameter. By placing the hot-wire such that only the prongs were in the flow field, measurements in the interior ($z = 7$ mm $> \delta \sim 2$ to 3 mm) could be obtained without greatly disturbing the flow. A maximum of six sensors could be used at one time; and signals were transmitted by rotating mercury contacts.

The analysis of the wave motions was done both on-line and in conjunction with a multi-channel tape recorder and an analog spectrum analyser. Both d.c.

and low-frequency amplifiers were available to amplify the anemometer output signals; and a pair of matched filters was used to isolate specific ranges of wave frequency. For on-line measurements, a pen recorder or oscilloscope was used, and frequencies were obtained by simple averages of the observed periods of oscillation.

To study the rod-induced waves, a single rod, as long as the fluid was deep, was placed at various radii (rod position r_R = 0·320, 0·410, 0·574 and 0·738) and system parameters (volumetric flux S and rotation frequency Ω) were adjusted so that there was an azimuthally propagating disturbance. The magnitude of the azimuthal perturbation velocity was measured at various positions relative to the disturbing rod; and phase measurements between various sensors were made. This was done by using the matched filters to isolate the fundamental wave frequency, and measuring the time lag between sensor signals with a chart recorder. The extended probe support could be used to measure the mean velocity in the wake of the disturbing rod, and mean velocity profiles for cases when no disturbing rod was present. Care had to be exercised to avoid disturbing effects associated with the extended probe support, and a discussion of the difficulties encountered can be found in Cerasoli (1974). A vertical traverser was available to change the length of the disturbing rod or to traverse a sensor and measure the axial structure of the disturbances associated with a disturbing rod. Again, care had to be exercised to avoid disturbing effects due to the probe support.

3. Experimental findings

Mean velocity. Before discussing the rod-associated wave motions, a few remarks about the mean azimuthal velocity in the absence of a disturbing rod are in order. Extensive mean azimuthal velocity measurements were made, using the extended probe support for the interior flow region and the side-wall boundary layers. The results of these measurements are in fair agreement with theoretical predictions made by Hide (1968) and Bennetts & Hocking (1973). It was found that, for the parameter range investigated $S \simeq 1000$–2200 cm^3 s^{-1}, $\Omega \simeq 3$–6 rad s^{-1}, the relative circulation $\Gamma = rV$ was approximately constant, and about 90–100 % of the theoretical value $\Gamma_{\text{th}} = S/2\pi\delta$. The extended probe support could give rise to azimuthally travelling disturbances, and this placed constraints on making measurements; the data reported in Cerasoli (1974) were free of such disturbances.

Wave characteristics. It was found that the frequency of the rod-associated disturbances was a function of the system Rossby number ($\epsilon_s = S/2\pi R_0^2 \delta\Omega$, outer radius R_0) and was independent of the disturbing rod diameter d for d = 1·6–4·8 mm. Figure 3 shows data taken for fixed Ω and a disturbing rod placed at r_R = 0·32. The linear relationship between wave frequency ω and volumetric flux S (which is proportional to ϵ_s for fixed Ω) is evident, and each straight line corresponds to an azimuthal wavenumber of the disturbance. For a given flux, either m = 2 or 3 could be obtained, depending on the manner in which the system parameters were realized. That is, at the onset of the

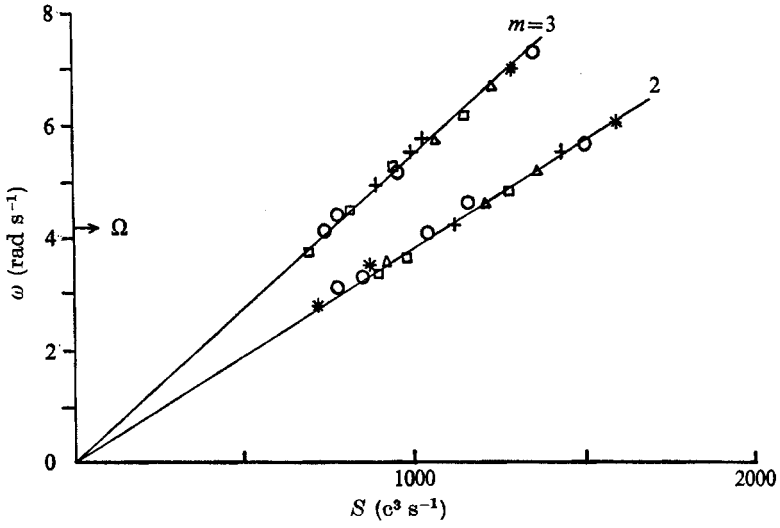

FIGURE 3. Disturbance frequency as a function of flux for fixed rotation rate and disturbing rod position 0·32, 19·6 cm. Disturbances with azimuthal wavenumbers $m = 2$ and 3 were observed. $\Omega = 4{\cdot}30$ rad s^{-1}.

Rod diameter (mm)	1·6	2·4	3·1	4·0	4·8
	+	△	○	□	*

disturbance, a mode with $m = 2$ was present, and a gradual increase in flux would retain the $m = 2$ mode. A great increase in flux could result in the $m = 3$ mode, and subsequent gradual changes in flux would retain the $m = 3$ mode. It should be pointed out that, typically, only one distinct mode was present in the final state, although a period may exist where both modes are competing. Only in a few out of many experiments was it found that two distinct modes existed in the final state.

The definition of an *azimuthal wavenumber* should be clarified. For a geometry with azimuthal symmetry, one can always decompose azimuthally travelling disturbances into modes given as exp $[i(m\phi - \omega t)]$. For such modes, m can be measured by placing two sensors at the same radius and separated by an angular distance $\Delta\phi$. Measurement of the time lag τ between sensors is related to m by

$$m = \frac{\omega\tau}{\Delta\phi} \pm \left[\frac{2\pi}{\Delta\phi}\right] N, \quad N = 0, \pm 1, \pm 2, \ldots. \tag{3.1}$$

The term $[2\pi/\Delta\phi]N$ arises from the inability to distinguish a phase shift $\Delta\Phi\,(= \omega\tau)$ from $\Delta\Phi \pm 2\pi N$. In an azimuthally symmetric geometry, m will always be an integer to satisfy periodicity.

The present experimental situation does not possess azimuthal symmetry. The disturbances are associated with the wake downstream from the disturbing rod, and this wake decays with increasing azimuthal distance. It was found that, defining m by use of (3.1), integer values were always obtained (to within experimental error in measuring τ). The azimuthal wavenumber, as defined by (3.1), was also found to be independent of the position of the sensors with respect to the disturbing rod.

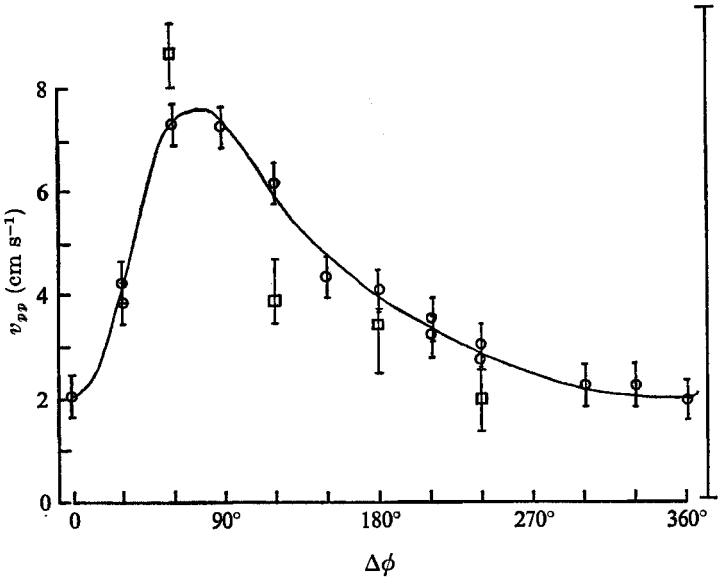

FIGURE 4. Azimuthal velocity of disturbance as a function of azimuthal distance from the disturbing rod (○). Rod position, 0·32. Sensor radius, 0·33. □, estimate of restoring force $s/l_{\frac{1}{2}}^3$ in the wake obtained from data shown in figure 8.

The amplitude of the disturbance did depend on the azimuthal distance from the disturbing rod; and figure 4 shows the azimuthal perturbation velocity as a function of this distance. The system parameters for these data were $\Omega = 4{\cdot}30$ rad s^{-1}, $S = 970$ c^3 s^{-1}, $\omega = 4{\cdot}12$ rad s^{-1} and $r_R = 0{\cdot}32$. The mean velocity V near the sensors (r sensor $= 0{\cdot}333$) was approximately 40 cm s^{-1} and the maximum percentage peak-to-peak fluctuations v_{pp}/V were approximately 20 %. The amplitude of the disturbance was large as the flux of 970 c^3 s^{-1} was about $1\frac{1}{2}$ times the critical flux at which the disturbance first appeared.

The data obtained on wave magnitude and azimuthal wavenumber demonstrate that the disturbances take the form $|f(\phi)| \exp[i(m\phi - \omega t)]$, where $|f(\phi)|$ does not contribute to the phase of the disturbance. Green and Green & Mollo-Christensen also observed integer wavenumbers using (3.1) in a similar experiment, although their interpretation of the disturbances was different.

Inspection of the data on frequency against Rossby number shows that, if an angular phase velocity is defined as $\dot{\phi}_{ph} = \omega/m$, $\dot{\phi}_{ph}$ is equal to the mean angular velocity V_R/r_R near the radius at which the disturbing rod is placed. That is,

$$\omega/m \simeq V_R/r_R, \tag{3.2}$$

where $V_R = V(r_R)$. Defining a non-dimensional wave frequency as $\omega_{nd} = \omega/\Omega$, and using the theoretical expression for $V_R = S/2\pi r_R \delta$, one has

$$\omega_{nd} \simeq m \frac{S}{2\pi r_R^2 \delta \Omega} = m\epsilon_R \quad \text{or} \quad \omega_{nd} = \beta m \epsilon_R. \tag{3.3), (3.4}$$

$\epsilon_R = V_R/(r_R\Omega)$ is a local Rossby number; β is approximately one.

The validity of (3.4) can be seen in figure 5. A single disturbing rod 3·2 mm in diameter was placed at one of the four radial positions $r_R = 0{\cdot}32$, 0·41, 0·57

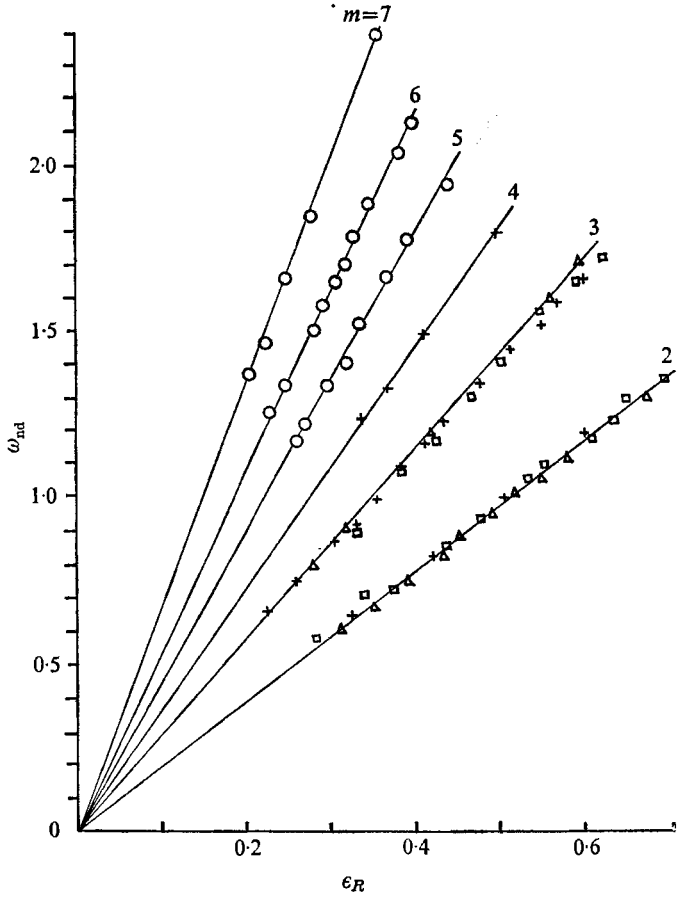

FIGURE 5. Non-dimensional disturbance frequency ω/Ω as a function of local Rossby number $S/2\pi r_R^2\delta\Omega$. Rotation rates 2·87, 4·30 and 6·08 rad s^{-1}. Disturbances with azimuthal wavenumbers m = 2–7 observed.

Rod position	0·32	0·41	0·57	0·74
	△	□	+	○

and 0·74; and three rotation rates were used, Ω = 2·87, 4·30 and 6·08 rad s^{-1}. Inspection of the data shows that m = 2 and 3 modes could be obtained for r_R = 0·32 and 0·41; m = 3 and 4 occurred for r_R = 0·57; m = 5, 6 and 7 for r_R = 0·74. Again, in the final state only one distinct mode was present in practically all the experiments.

As stated previously, the phase shift between two sensors at the same radius and separated by $\Delta\phi$ was found to be $\Delta\Phi = m\Delta\phi$. For two sensors at the same azimuthal position but at different radii, the phase difference was as follows. For both sensors at radii either less or greater than r_R, the signals were in phase. For one sensor at $r > r_R$ and the other at $r < r_R$, the signals were 180° out of phase.

The magnitude of v was uniform with axial position; this is to be expected, as the disturbing rod was as long as the annulus was deep. Some experiments

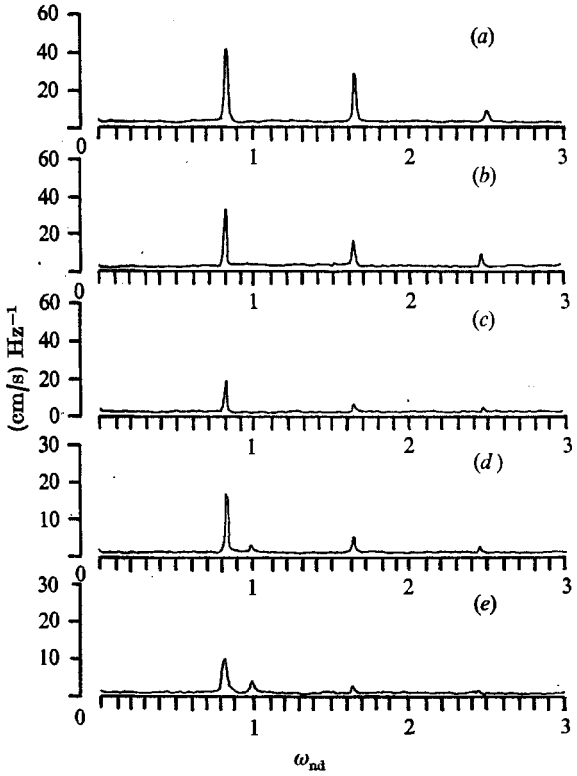

FIGURE 6. Wave spectra for azimuthal component of disturbance at various non-disturbing sensors for rod position $r_R = 0{\cdot}41$, $\phi_R = 90°$, $S = 1365$ c^3 s^{-1}, $\Omega = 4{\cdot}30$ rad s^{-1}, $m = 2$.

	(*a*)	(*b*)	(*c*)	(*d*)	(*e*)
r	0·333	0·333	0·333	0·500	0·667
ϕ (deg)	180	0	60	60	60

were done placing a disturbing rod halfway into the annulus. If the rod extended from $z = 0$ to $\frac{1}{2}H$, where H is the annulus depth, it was found that the wave amplitude was approximately uniform for $z = 0$ to $\frac{1}{2}H$ and diminished in the region from $z = \frac{1}{2}H$ to H. The difference in amplitude between $z = 0$ and H was typically an order of magnitude. In all cases, whether or not the rod extended throughout the annulus, no phase variations existed along the axial direction.

Measurements were made with sensors at the same azimuthal angle, and at various radii. It was found that the wave amplitude was greatest in the vicinity of r_R, and decayed with increasing distance from it. Thus, the data suggest that the rod-associated disturbances were azimuthally propagating waves with the greatest amplitude at radii near r_R, and about 60° downstream from the disturbing rod (see figure 4). When the rod was as long as the annulus was deep, the disturbances had no vertical structure.

Figure 6 shows spectra for a typical disturbance. The rod was at $r_R = 0{\cdot}41$ and $\phi_R = 90°$; the spectra at $r = 0{\cdot}333$ are presented in the order of increasing azimuthal distance from ϕ_R. The signals at $r = 0{\cdot}333$, $\phi = 60°$ and $r = 0{\cdot}500$,

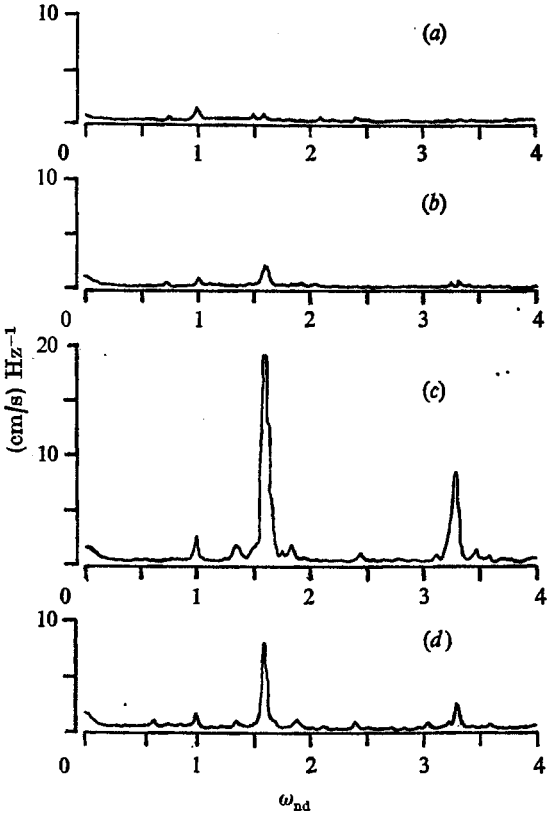

FIGURE 7. Similar to figure 6, except that $r_R = 0{\cdot}74$, $\phi_R = 90°$, $S = 3050$ c^3 s^{-1}, $m = 6$.

	(a)	(b)	(c)	(d)
r	0·333	0·500	0·667	0·833
ϕ (deg)	60	60	60	60

$\phi = 60°$ were 180° out of phase; those at $r = 0{\cdot}500$, $\phi = 60°$ and $r = 0{\cdot}667$, $\phi = 60°$ were in phase. The vertical scale is in units of (cm/s) Hz^{-1} (v_{pp}/Hz); and, as the typical width of a spectral peak is about 0·05 Hz, v_{pp} can be estimated by multiplying the vertical scale by 0·05 Hz. The decrease in wave amplitude with increasing radial distance from r_R can be seen; the change in vertical scale for $r = 0{\cdot}500$ and 0·667 should be noted. The low-level signal at $\omega_{nd} = 1{\cdot}0$ for $r = 0{\cdot}500$ and 0·667 is system noise at the rotation frequency. (It is not seen at $r = 0{\cdot}333$, because of the high signal-to-noise ratio.) It amounted typically to less than 0·2 % p.p. of the ambient velocity. Figure 7 shows spectra for $r_R = 0{\cdot}74$, $\phi_R = 90°$. The signals at $r = 0{\cdot}667$ and 0·833 were out of phase; those at $r = 0{\cdot}500$ and 0·667 were in phase. It should be noted that the sensors were at $\phi = 60°$, and were 30° *upstream* of the disturbing rod.

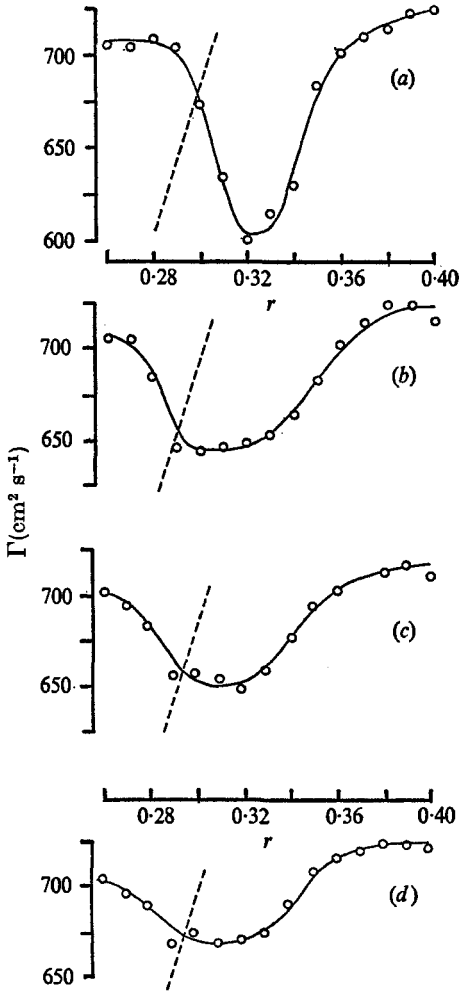

FIGURE 8. Circulation profiles in vicinity of $r_R = 0{\cdot}32$ as a function of increasing azimuthal distance from disturbing rod. Intersection between two curves marks the radius at which wave phase velocity equals mean azimuthal velocity. – – –, radius times wave phase velocity ($r^2\omega/m$).

	(*a*)	(*b*)	(*c*)	(*d*)
$\Delta\phi$ (deg)	60	120	180	240
s	0·18	0·11	0·10	0·07
$l_{\frac{1}{2}}$	0·04	0·06	0·06	0·07

4. Wake structure and measurement technique

A number of the disturbance properties are similar to what is expected for a wake instability; the most obvious being the matching of wave phase velocity with mean velocity in the vicinity of r_R. Measurements were made on the wake downstream from the disturbing rod, using the extended probe support. As this probe support can create a number of disturbance effects, a discussion of its use will follow the statement of experimental results.

A disturbing rod, 3·2 mm in diameter, was placed at $r_R = 0{\cdot}32$ and four

distinct azimuthal positions such that, when the radial position of the extended support sensor r_S was at 0·32, the azimuthal separations $\Delta\phi$ between r_R and r_S were 60, 120, 180 and 240°. S and Ω were 970 c^3 s^{-1} and 4·30 rad s^{-1}, respectively, and a disturbance with $m = 2$, $\omega_{\mathrm{nd}} = 0{\cdot}96$ was present. The extended support sensor was traversed into the wake, and mean velocities were measured. Figure 8 shows the circulation profiles at the four azimuthal separations, and the decay of the wake can be seen. The wake strength s (fractional decrease in circulation) and wake half-width $l_{\frac{1}{2}}$ have been estimated from the profiles. The dashed curves are radius times the measured wave phase velocity, and are equal to $r^2\omega/m$. The matching of wave phase velocity and mean velocity is represented by the intersection of $r^2\omega/m$ and $\Gamma(r)$.

The measurement of wake structure with the extended probe is subject to a number of criticisms concerning disturbing effects due to the extended probe support (Fultz & Kaiser 1971). To justify this set of measurements, a discussion of such disturbance effects will be presented. First, the use of the extended support in the *absence* of a disturbing rod will be considered. The extended support consists of a vertical section of rod at $r = 0{\cdot}58$, which extends halfway into the annulus, and a horizontal section approximately 26 cm long. Both sections of support will produce wakes, and can give rise to disturbances. A disturbance associated with the vertical section of the support will be similar to the wave motions discussed in this paper. Disturbances due to the wake of the horizontal section of the support are more complicated: an example will be given. For system parameters $S = 2500$ c^3 s^{-1} and $\Omega = 4{\cdot}30$ rad s^{-1}, no disturbances were present with the extended support sensor near the outer radius $r_S \simeq 1{\cdot}0$. The sensor was traversed radially inward to regions of higher azimuthal velocity and at $r_S \simeq 0{\cdot}35$ a disturbance was detected. As r_S was decreased further, the frequency of the disturbance increased. Traversing the sensor back to $r_S \simeq 0{\cdot}35$ caused the observed signal to decay. For $S = 1500$ c^3 s^{-1}, $\Omega = 4{\cdot}30$ rad s^{-1}, no such disturbances were observed for any r_S; and it is safe to say the wakes from both sections of the support were stable.

For the situation when a disturbing rod and related disturbance were present, the extended support presented a number of other difficulties. Initially, the wake associated with a disturbing rod at $r_R = 0{\cdot}41$ was studied. System parameters were adjusted so that a rod-associated disturbance with $m = 2$ was present and the extended support was *not* in the annulus. The extended probe was placed in the annulus with $r_S \simeq 1{\cdot}0$; and repeating the experiment with the same parameters gave rise to the same $m = 2$ disturbance (as measured at the non-disturbing probes). It was found that traversing the sensor into the wake, $r_S \simeq r_R$, caused the $m = 2$ mode to decay, and a mode with $m = 3$ to appear. Traversing the sensor to $r_S > r_R$ would cause the $m = 3$ mode to decay, and the $m = 2$ mode to grow. This behaviour was repeatable, and it appears that interfering with the wake caused the most unstable mode to change from $m = 2$ to $m = 3$. When the previous technique was applied to a disturbing rod at $r_R = 0{\cdot}32$ and a value of flux well above the critical ($\sim 1\frac{1}{2}$ times), a mode with $m = 2$ was retained independent of r_S. Even for this case, disturbing effects due to the extended support were observed. For measurements at $\Delta\phi = 60$,

	Ω (rad s^{-1})				
r_R	1·88	2·87	4·30	6·08	7·44
0·32	0·60	0·45	0·35	0·25	0·21
0·41	0·59	0·44	0·33	0·25	0·21
0·57	0·53	0·39	0·30	0·23	0·19
0·74	0·50	0·38	0·29	0·22	0·18

TABLE 1. Critical Rossby number as a function of disturbing rod position and rotation rate for rod diameter of 3·2 mm

120 and 180°, a small decrease ($\sim 10\,\%$) in wave amplitude and frequency was observed at the non-disturbing sensors as the sensor was traversed into the wake. At $\Delta\phi = 240°$, the decrease in amplitude became substantial ($\sim 40\,\%$), while the frequency still decreased by about 10 %.

The disturbing effects discussed for the data presented in figure 8 are not believed to invalidate that data. The estimated values of s and $l_{\frac{1}{2}}$ are not as accurate as one would want; but the data do show wake decay, and give one a handle on the wake parameters.

5. Onset data

The critical local Rossby number was measured for the onset of the rod-associated disturbances. The rotation rate was fixed, and the volumetric flux increased until a disturbance grew out of the noise, which was about 0·1–0·2 % p.p. of the ambient velocity. The critical Rossby number was defined as $\epsilon_c = S_c/2\pi r_R^2 \delta\Omega$, where S_c was the volumetric flux at which disturbances were observed. Hysteresis effects similar to those reported by Ingram (1971) were observed; if S_c were the flux for initiating a disturbance, one could go to $S < S_c$ and the wave would persist. Typically the disturbance would decay for $S \sim 0{\cdot}90 S_c$.

Some onset data are presented in table 1; the disturbing rod was as long as the annulus was deep, and the rod diameter d was 3·2 mm. For fixed Ω, ϵ_c depends weakly on r_R, indicating that $(V_R)_{\text{crit}}$ is approximately proportional to r_R; for fixed r_R, ϵ_c depends strongly on Ω. Busse (1968) studied the stability of azimuthally symmetric shear flow in rotating co-ordinates, and found that the ratio $\epsilon_c/E^{\frac{1}{2}}$ should be constant at onset ($E = \nu/H^2\Omega$). Physically, this represents a balance between energy input to the disturbances from the mean shear and wave dissipation due to Ekman pumping. In the present experiment, the wake decays downstream from the rod and the ratio $\epsilon_c/E^{\frac{1}{2}}$ need not be constant. This was found to be the case.

The onset data are qualitatively consistent with the assumption that a circulation deficit or wake must extend completely around the annulus for disturbances to propagate. For fixed Ω and d, $(V_R)_{\text{crit}}$ increased with increasing r_R, and for fixed Ω and r_R, $(V_R)_{\text{crit}}$ decreases as d increases, which is consistent with a wake deficit increasing as d increases. For fixed r_R and d, $(V_R)_{\text{crit}}$ increases

d (mm)	ϵ_c	Re_R	
1·6	0·45	40	No von Kármán vortices present
2·4	0·39	50	
3·2	0·35	60	Von Kármán vortices present
4·0	0·34	74	
4·8	0·32	84	

TABLE 2. Critical Rossby number as a function of disturbing rod diameter for $r_R = 0{\cdot}32$ and $\Omega = 4{\cdot}30$ rad s^{-1}. Reynolds numbers based on the theoretical velocity and rod diameter are also listed.

with increasing Ω, which is consistent with increased dissipation for both the wake and the wave motions as Ω increases.

Data for various rod diameters were obtained; and ϵ_c as a function of d is listed in table 2. The onset mechanism is independent of the high-frequency von Kármán vortex streets (typically 5–15 Hz) that occur downstream from the rod for a rod Reynolds number $V_R d/\nu$ greater than about 50. Low-frequency disturbances occurred with and without vortex streets present; and situations existed where vortex streets were present and no low-frequency disturbance was observed. It was found that the von Kármán streets decayed substantially over distances of about 20–30 cm.

A few remarks about onset are in order. First, the criteria used in these experiments required that the disturbances be above the ambient noise level. This meant that very low-level disturbances would go undetected, and the values obtained for ϵ_c are for finite-amplitude waves and overestimate the true critical Rossby number. At onset, usually two modes were present, giving rise to a highly modulated signal. There was a transient period while the two modes had nearly equal amplitudes; but eventually the mode with the lower m would supersede the higher m mode. For a given rod position, the wave-numbers of the initial modes were the same with varying Ω, and there was an interesting relationship between wave frequency ω and rotation rate. This was that ω/Ω was always given by N/M, where N and M are integers. This feature was detected by simultaneously observing ω and Ω.

The above statements can be clarified by considering onset data for $r_R = 0{\cdot}32$. Modes with $m = 2$ and 3 were observed initially; and the $m = 2$ mode became the final one. The non-dimensional frequencies at onset were $\omega_{\mathrm{nd}} = \frac{5}{6}, \frac{2}{3}$ and $\frac{1}{2}$ for $\Omega = 2{\cdot}87$, $4{\cdot}30$ and $6{\cdot}08$ rad s^{-1}, respectively. The relationship between ω and Ω suggests that the disturbances are being forced in some manner by noise at the rotation frequency. Ratios of $\omega/\Omega = \frac{1}{2}, 1, 2 \ldots$ might be explained by a simple parametric resonance process; but ratios such as $\frac{2}{3}$ or $\frac{5}{6}$ would not occur in this. No explanation is presented for the phenomena; the experimental facts are stated for completeness.

A transient period was also observed by Ingram in similar experiments: he states that spectra were not taken until 15 min after changing system parameters. In the present experiment, the transient period could last for as long as 5 min. Ingram presented a large amount of spectral data, but no absolute

magnitude information; and this makes comparison with the present experiment difficult. Inspection of Ingram's spectra for a very low ϵ_R (most probably near onset, although no data are presented concerning onset) show that ω_{nd} is also of the form N/M.

The onset data presented to this point had the disturbing-rod length L equal to the plate separation H. It was found that the critical Rossby number was very sensitive to L; and the following behaviour was observed. For $\epsilon \simeq \epsilon_c$ and $L = H$, a small decrease in L (~ 6 mm or $\sim 2\delta$) caused the disturbance to decay (as observed at the non-disturbing sensors). When ϵ was increased the disturbance would persist for smaller values of L. This is obvious, as the amount of shear in the flow field decreases as L decreases; but it is relevant to a comparison of the present work with the work of Tatro & Mollo-Christensen and Tatro. If the disturbing rod were a hot-wire probe support and $\epsilon \simeq \epsilon_c$, traversing the sensor upward would cause the disturbance to decay, and could be interpreted as an Ekman instability confined to the boundary layer. Similarly, for $\epsilon > \epsilon_c$, the persistence of the disturbance as the sensor was traversed out of the boundary layer could be interpreted as inertial waves propagating into the interior.

6. The wake instability in cylindrical geometry

The linearized, inviscid equations for two-dimensional disturbances in rotating co-ordinates were studied to gain some insight into the nature of the rod-associated disturbances. The mean velocity V relative to the rotating co-ordinates was azimuthal and axisymmetric, and the non-dimensional equations in cylindrical co-ordinates are

$$-i(\omega - \epsilon m V/r)u - 2(1+\epsilon V/r)v = -p', \tag{6.1}$$

$$-i(\omega - \epsilon m V/r)v + 2(1+\epsilon(rV)'/2r)u = -imp/r, \tag{6.2}$$

$$(ru)' + imv = 0. \tag{6.3}$$

The perturbation is of the form $f(r)\exp[i(m\phi - \omega t)]$; and u, v and p are the perturbation radial velocity, azimuthal velocity and pressure, respectively. Lengths have been scaled by R_0, time by Ω^{-1} and velocity by $\epsilon R_0 \Omega$; primes denote differentiation with respect to radius. Combining (6.1)–(6.3), one obtains

$$\xi'' + \frac{\xi'}{r} + \left(-\frac{m^2}{r^2} + \frac{\epsilon m r^{-1}(\Gamma'/r)'}{\omega - \epsilon m \Gamma/r^2}\right)\xi = 0. \tag{6.4}$$

$\xi = ru$, and $\Gamma = rV$ is the circulation relative to the rotating co-ordinates. Equation (6.4) is similar to the one derived by Busse (1968), although his analysis allowed for variable depth and dissipation due to Ekman pumping. The dissipation can be included by replacing $\epsilon m\Gamma/r^2$ by $\epsilon m\Gamma/r^2 - 2iE^{\frac{1}{2}}$; and it is equivalent to damping given by $\exp[-2E^{\frac{1}{2}}t]$. In this paper, the inviscid equation (6.4) will be studied; and $2E^{\frac{1}{2}}$ will be used to estimate dissipation due to Ekman pumping. It should be noted that the rotation of co-ordinates Ω appears in (6.4) only in defining ϵ: this is a consequence of dealing with two-dimensional disturbances.

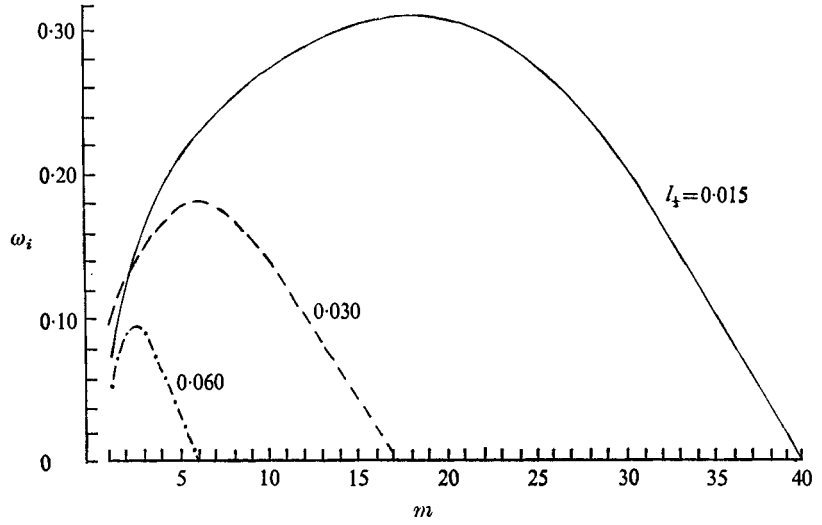

FIGURE 9. Growth rate as a function of azimuthal wavenumber for azimuthally symmetric wakes of fixed strength $s = 0{\cdot}20$, position $r_R = 0{\cdot}32$ and varying half-widths $l_{\frac{1}{2}}$.

Equation (6.4) is similar to the well-known Rayleigh stability equation for plane parallel flow, and the term $(\Gamma'/r)'$ plays the role of U'' in the Rayleigh problem. It can easily be shown that

$$\operatorname{Im}\omega \int_{R_I}^{R_O} \frac{(\Gamma'/r)'}{|\omega - em\Gamma/r^2|^2} |\xi|^2 dr = 0. \tag{6.5}$$

R_I and R_O are the inner and outer radii. For unstable modes, $(\Gamma'/r)'$ must change sign, and the relative circulation must possess an inflexion point.

The relative circulation for a rotating source–sink annulus has no radial inflexion points when disturbing rods are not present, and the flow field is stable to this class of two-dimensional disturbances. The situation is different when a disturbing rod, or probe support, is introduced. The circulation profile in the wake of the rod possesses radial inflexion points, and can be unstable.

The eigenvalue problem of (6.4) was solved using the 'shooting method'. (See Fox 1959.) A numerical grid of 1000 points between $R_I = 0{\cdot}188$ and $R_O = 1{\cdot}000$ was used; and the boundary conditions were $\xi = 0$ at $r = R_I, R_O$. The circulation profile was taken to be

$$\Gamma(r) = 1 - s[\operatorname{sech} K(r - r_R)]^2. \tag{6.6}$$

s is the strength of the wake; K is related to the half-width $l_{\frac{1}{2}}$ by

$$K = 1{\cdot}76/l_{\frac{1}{2}}.$$

Far from the wake, the circulation was constant, and vertical side-wall boundary layers were not included for the mean velocity. Some calculations were done including side-wall layers: the results did not change significantly for the values of r_R considered.

Figure 9 is a plot of calculated growth rate ω_i against azimuthal wavenumber for fixed wake position r_R, strength s and varying half-width $l_{\frac{1}{2}}$. The real part

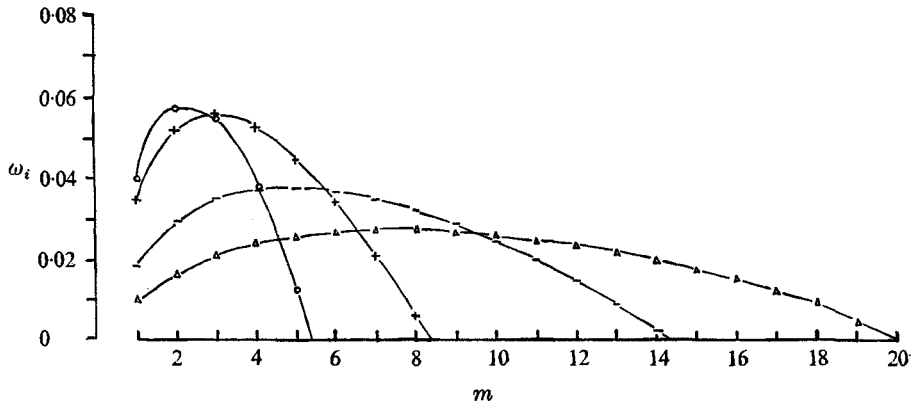

FIGURE 10. Similar to figure 9, except that $s = 0{\cdot}10$ and $l_{\frac{1}{2}} = 0{\cdot}06$.

r_R	0·32	0·41	0·57	0·74
	○	+	−	△

of ω is always approximately $\epsilon m V_R/r_R = m\epsilon_R$, which corresponds to a matching of phase velocity with mean velocity in the vicinity of the wake. The most unstable wavenumber decreased for increasing $l_{\frac{1}{2}}$; the growth rate of that mode decreased due to the decreasing shear in the wake. The relevant result is that, for a broad wake ($l_{\frac{1}{2}} = 0{\cdot}06$), low-wavenumber modes ($m = 2, 3$) are the most unstable. The results for a 'thin' wake ($l_{\frac{1}{2}}/r_R \ll 1$), where curvature effects are small, are similar to those for the plane parallel flow problem. (See Betchov & Criminale 1967, p. 39.) Figure 10 shows the effect of placing an axisymmetric wake at various radii; for increasing r_R, higher values of the most unstable wavenumber are obtained. This is consistent with experimental results, observing higher values of m for increasing r_R.

The unstable modes found in this computation are analogous to the symmetric modes of the plane parallel flow problem (Betchov & Criminale *loc. cit.*): figure 11 shows perturbation velocities for a typical wake instability. The phase shift across the wake of approximately 190° for v compares favourably with the experimentally observed value of 180°.

The wake produced by the disturbing rod is not axisymmetric, as shown in figure 8. To gain some understanding of a the effect of decaying wake, curves representing ω_i against m were computed for *axisymmetric* wakes with the experimental wake parameters of figure 8. These results are shown in figure 12; a dissipation frequency has been estimated by $2E^{\frac{1}{2}}(\Omega \simeq 4{\cdot}30 \text{ rad s}^{-1})$. During the experiments on wake structure, a mode with $m = 2$ and $\omega_{\text{nd}} = 0{\cdot}96$ was present. It is interesting that, for an axisymmetric wake with the parameters for wakes at $\Delta\phi = 120$ and 180°, $m = 2$ is the most unstable mode.

The results of the preceding calculation have a number of features in common with the experimental findings. These are as follows. (i) The wave phase velocity matches with the mean velocity in the vicinity of the wake. (ii) For fixed wake parameters and increasing r_R, the azimuthal wavenumber of the most unstable mode increases. (iii) The computed phase shift for v across

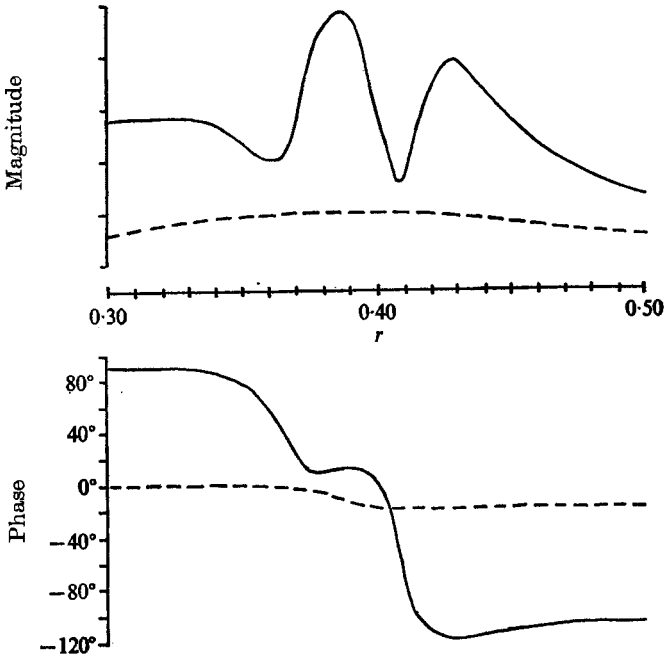

FIGURE 11. Magnitude and phase of radial and azimuthal perturbation velocities for a typical unstable mode. The complex phase velocity $c = m\omega$ (= 1·153, 0·153) has been normalized by the mean velocity at the disturbing rod radius. $r_R = 0{\cdot}41$, $s = 0{\cdot}10$, $l_{\frac{1}{2}} = 0{\cdot}06$, $m = 2$. ---, ru; ——, v.

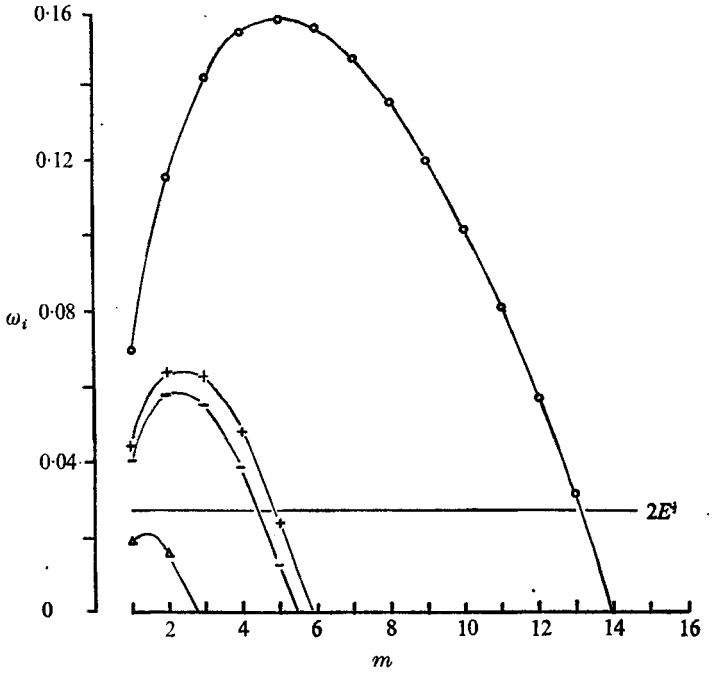

FIGURE 12. Growth rate as a function of azimuthal wavenumber for $r_R = 0{\cdot}32$ and wave parameters taken from the data presented in figure 8.

	○	+	−	△
s	0·18	0·11	0·10	0·07
$l_{\frac{1}{2}}$	0·04	0·06	0·06	0·07

the wake agrees well with the measured values. (iv) The most unstable mode for an axisymmetric wake, with parameters determined in the slowly decaying region ($\Delta\phi = 120$–$180°$), agrees with the observed mode.

The observation that in nearly all the experiments a single mode (azimuthal wavenumber) was present, not a distribution of wavenumbers, suggests that the wake instability was forced. Inspection of a typical calculated curve of growth rate against m (see figure 10) shows that one might expect a single mode to be present for small r_R ($= 0{\cdot}32$), but certainly not for large r_R ($= 0{\cdot}74$), where the curve is broad and relatively flat in the vicinity of the most unstable wavenumber. The source of the forcing is believed to be noise at the rotation frequency. Although care was taken to align the annulus and use high-quality bearings, a small signal at the rotation frequency could always be detected; such a signal was consistent with small fluctuations of the rotation rate ($\sim 0{\cdot}05\,\%$ p.p. of Ω). It is believed that this 'Ω' noise forced the wake instability in some unspecified, nonlinear fashion, as mentioned in the discussion of onset data. This would also be consistent with the fact that wave frequencies were always the same order of magnitude as the rotation frequency. Another observation consistent with forcing is that one case where two modes were observed in the final state was for $r_R = 0{\cdot}32$ with $m = 2$, $\omega_{\mathrm{nd}} = \frac{2}{3}$ and $m = 3$, $\omega_{\mathrm{nd}} = 1{\cdot}00$. It should be noted that, although not discussed by other workers (Caldwell & Van Atta 1970; Ingram 1971), energy near the rotation frequency can be seen in the spectra presented by them.

The azimuthal dependence of the perturbation velocity can be explained in terms of the 'restoring force' $(\Gamma'/r)'$. As the wake decays with increasing azimuthal distance from the disturbing rod, $(\Gamma'/r)'$ decreases, and its magnitude can be estimated as $s/l_{\frac{1}{2}}^2$. This quantity has been plotted in figure 4, and a similarity in both v_{pp} and $s/l_{\frac{1}{2}}^2$ as a function of azimuthal angle can be seen.

7. Comparison with previous experiments

The interior wave motions reported by Green (1968), Green & Mollo-Christensen (1970) and Ingram (1971) have properties very similar to the rod-associated waves observed here: figure 13 shows data taken from that literature. In these experiments, a hot-wire sensor was placed at the mid-depth in the annulus, which resulted in a disturbing rod extending half-way through the annulus. The non-dimensional frequency is plotted against the system Rossby number

$$(\epsilon_R = \epsilon_s/r_R^2);$$

and, if one assumes that the waves were rod-induced, β and m for Green, and Ingram's data are consistent with data obtained in the present experiment.

The linear relationship between wave frequency and Rossby number observed in the data is one that extrapolates to $\omega = 0$ with Rossby number. Such behaviour is consistent with rod-associated waves, since the velocity at the rod goes to zero as $\epsilon_R \to 0$. Inertial-wave frequencies would not extrapolate to zero as $\epsilon_R \to 0$, because the Coriolis restoring force does not vanish. Although Green and Ingram interpreted the interior waves as inertial modes, no measurements

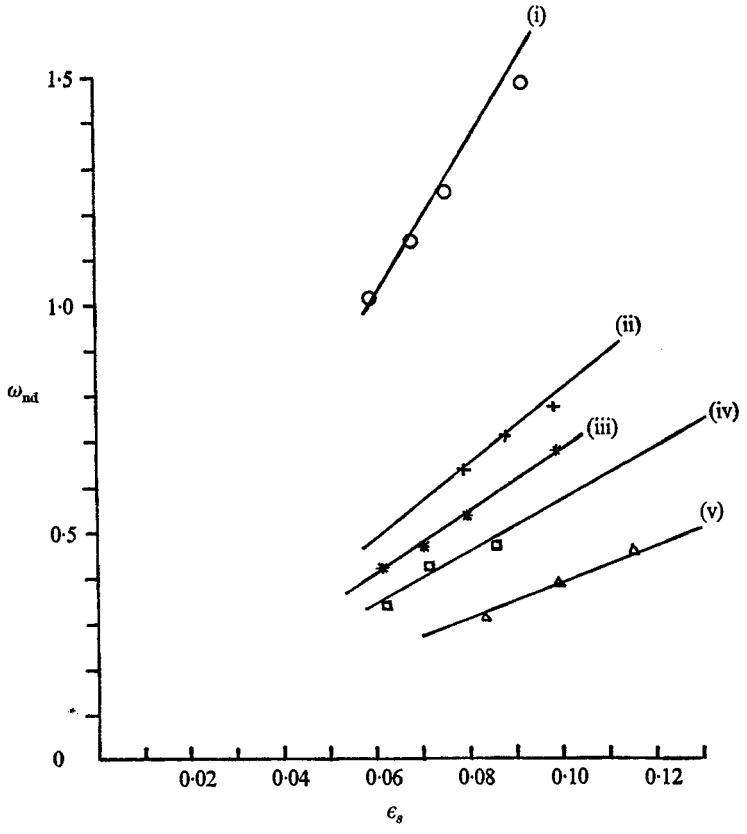

FIGURE 13. Non-dimensional frequency as a function of system Rossby number from (+) Green & Mollo-Christensen (1970) and (all other data) Ingram (1971).

	(i)	(ii)	(iii)	(iv)	(v)
m	2	3	3	3	3
β	0·76	0·88	0·96	0·90	0·90
Sensor radius	0·29	0·57	0·64	0·74	
	○	+	□	△	

on vertical wave structure were presented. Inertial modes in a closed annulus have v proportional to $\cos(N\pi z/H)$, where $N = 1, 2, \ldots$, and nodal points should be observable for true inertial modes.

The present study showed that probe supports can produce low-wavenumber, azimuthally propagating disturbances, and the wave motions, interpreted by Green and Ingram as inertial modes, were most likely rod-associated waves. Tatro & Mollo-Christensen (1967) used an annulus similar to that used in the present experiment; and it is likely that they, too, observed rod-induced waves. Data were taken in two ways in their experiment. A probe support extended from the upper plate, through the annulus into the Ekman layer near the lower plate. Thus, a disturbing rod was in the flow field. The other method employed non-disturbing probes, which extended either 3 or 6 mm from the boundary. One might assume that no disturbing rod was in the system during such experiments; but this was not the case. As reported in Tatro (1966), a 1 mm diameter

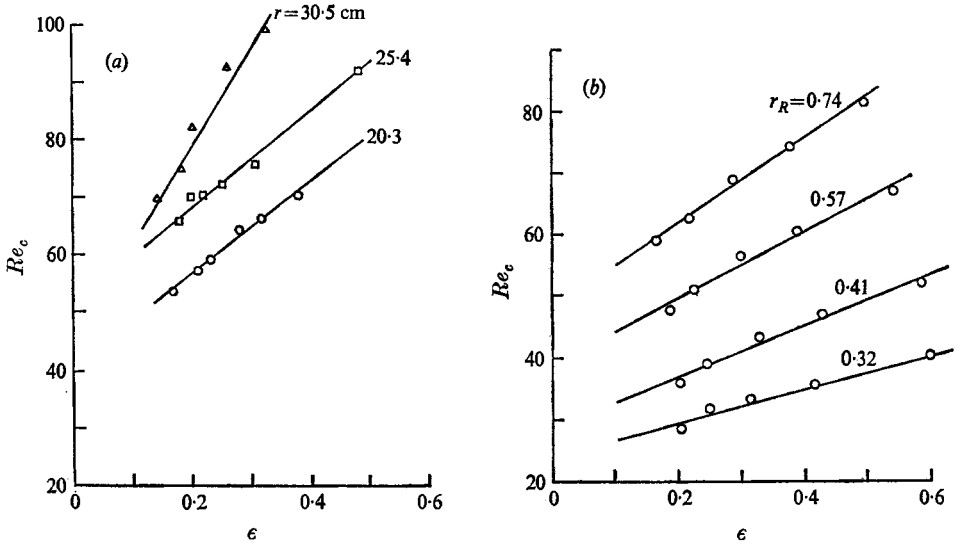

FIGURE 14. Critical Reynolds number $Re_c = S/2\pi r\nu$ as a function of Rossby number $\epsilon = S_c/2\pi r_R^2 \delta\Omega$ for (*a*) disturbances labelled type-II Ekman instabilities, from Tatro (1966), and (*b*) rod-associated disturbances. Rod diameter, 3·18 mm.

rod was placed at a small radius "to stimulate the instability". Tatro justified use of this by observing that wave frequencies were independent of rod diameter ($d \sim 1$–4 mm). This is precisely the behaviour observed for the rod-induced waves in the present experiment.

One of the better ways to distinguish Ekman instabilities from rod-associated waves is to have data on wave frequency against Rossby number. Unfortunately, Tatro & Mollo-Christensen and Tatro give no such data explicitly; and one must look to other data for comparison. Figure 14(*a*) is a plot of critical Reynolds number against local Rossby number from Tatro. The wave motion was interpreted as a type-II instability; and Re and ϵ are based on theoretical values for velocity and Ekman thickness $\delta = (\nu/\Omega)^{\frac{1}{2}}$. Tatro found that, defining Re and ϵ using measured values of velocity and Ekman thickness, the three curves of figure 14 would collapse into a single curve,

$$Re = 56{\cdot}3 + 116{\cdot}8\epsilon_L. \tag{7.1}$$

$\epsilon_L = V_m/2r\Omega$ and $Re = V_m\delta_m/\nu$; and subscripts m denote measured values.

Equation (7.1) has been criticized by Green & Mollo-Christensen, because of the manner in which boundary-layer thicknesses were obtained. The thicknesses were based on the height at which the voltage for a hot wire aligned parallel to the azimuthal velocity was a maximum. Such an orientation would have the hot wire sensitive to the radial component of the velocity U, and a correct measure of the position z at which U is a maximum is related to δ by $\delta = 4z/\pi$ for an Ekman profile. Green & Mollo-Christensen, using similar equipment, found that thicknesses obtained in this manner were artifacts of the hot-wire response to the vertical gradient of the azimuthal velocity and the

change in the mode of heat transfer near the boundary. For the data presented by Tatro to collapse onto a single curve, δ_m must increase with decreasing radius (no δ_m's are explicitly given by Tatro). Both Green (1968) and Caldwell & Van Atta found no radial dependence of δ_m. Finally, theoretical arguments by Faller & Kaylor (1966*a*) suggest an explanation of the dependence of the critical Reynolds number upon local Rossby number which does not predict a linear relationship between the two.

The preceding remarks lead one to rely only on the data presented in figure 14(*a*); and such behaviour is not expected for the type-II instability. Figure 14(*b*) shows data obtained in the present experiment for the onset of the rod-associated disturbances. A 3·2 mm rod was placed at four radii, and critical Re and ϵ were defined, based on theoretical velocities and Ekman thicknesses. These data bear a close resemblance to Tatro's, although the precise values of Re and ϵ do not agree. The critical Reynolds numbers obtained by Tatro are typically greater than those observed in the present experiment: this is believed to be due to at least two factors. First, the probe support used by Tatro had a diameter of 2·5 mm, as compared to the 3·18 mm rod used for the data shown in figure 14(*b*). As discussed in §5, the critical Reynolds number for rod-associated waves increases with decreasing rod diameter. Second, the construction of the hot-wire probes used by Tatro consisted of a 2·5 mm diameter rod with fine needles approximately 5 mm long holding the hot-wire sensor. When the sensor was placed in the boundary layer, the length of the disturbing rod in the flow field was the annulus depth minus approximately 5 mm. The present data were obtained with a disturbing-rod length equal to the annulus depth; and, as discussed in §5, the critical Reynolds number for rod-associated waves increases with decreasing rod length. Finally, the onset criterion used by Tatro is not given. In the present experiment, disturbances with amplitudes less than $\frac{1}{2}\%$ p.p. of ambient velocity (typically less than 0·15 cm s^{-1}) were detected. If the detection of disturbances by Tatro required amplitudes greater than were required in the present experiment, critical Reynolds numbers would also be greater. Tatro observed no disturbances below $Re \simeq 55$, which is the theoretically predicted critical Reynolds number for type-II instabilities. If the disturbances observed by Tatro were rod-associated waves, the factors discussed could have been responsible for none being observed below $Re \simeq 55$. The point is the similarity between the data shown in figures 14 (*a*), (*b*) and the fact that the different curves of Re against ϵ in figure 14(*a*) for different radii are neither the predicted behaviour for type-II waves, nor the observed (Faller & Kaylor 1966*b*; Caldwell & Van Atta 1970).

Tatro & Mollo-Christensen reported observing Ekman instabilities confined to the boundary layer for fluxes near the critical value, and wave motions propagating into the interior for fluxes exceeding the critical value. This behaviour can be seen in figure 15 from Tatro; the data were taken by placing a hot wire in the Ekman layer from above, and slowly traversing (0·127 mm s^{-1}) the sensor upward. The apparent confinement of the disturbance to the boundary layer for fluxes near critical value was taken as evidence that Ekman instabilities were being observed. As discussed in the section on onset data, the

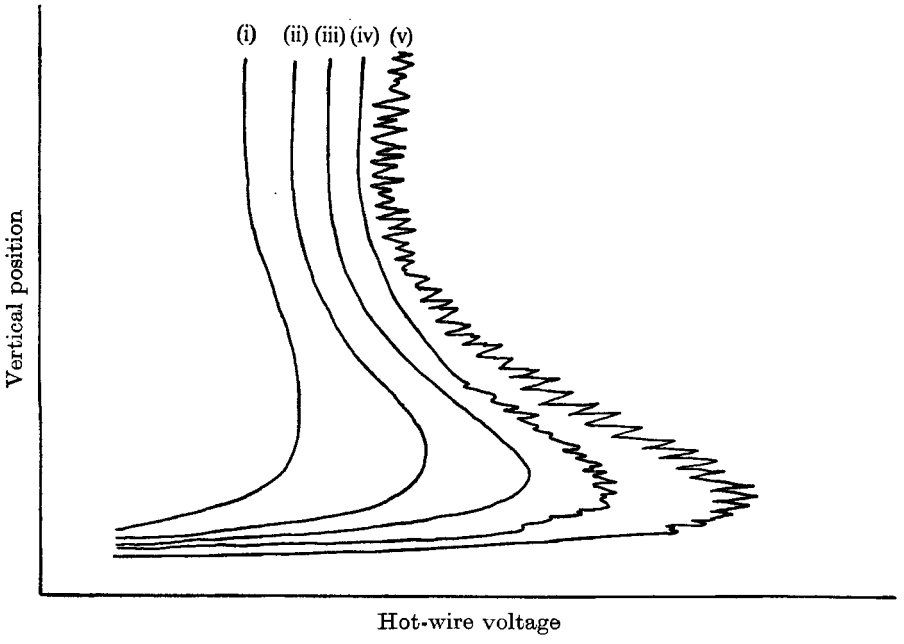

FIGURE 15. Hot-wire voltage as a function of vertical position of sensor for various values of flux, from Tatro (1966). $\Omega = 4{\cdot}0$ rad s^{-1}, $r = 25{\cdot}4$ cm.

	(i)	(ii)	(iii)	(iv)	(v)
S (c^3 s^{-1})	850	1200	1575	1925	2285

rod-associated waves depend strongly on rod length, especially when fluxes are near their critical value. The behaviour shown in figure 15 is similar to that observed in the present experiment, with the rod-induced waves persisting for shorter rod lengths as the flux is increased beyond the critical value. It should be noted that the oscillations of figure 15 do not imply vertical wave structure. The pattern is one which would be obtained by slowly traversing a sensor in a wave field which is uniform with height. The frequency of the disturbance is related to the pattern of figure 15 by

$$\text{frequency} = (\text{number of waves mm}^{-1}) \times (0{\cdot}127 \text{ mm s}^{-1}).$$

Using this relationship one obtains frequencies of order 1 Hz (also of the order of the rotation frequency); and this is consistent with other frequency data given by Tatro.

The frequency of the disturbances observed by Tatro & Mollo-Christensen was typically of the order of the rotation frequency. Such frequencies are an order of magnitude smaller than what is expected for a type-II instability, and are more consistent with frequencies observed for rod-induced waves. Tatro did not explicitly present data on frequency against Rossby (or Reynolds) number; but Tatro (1966, figure 3·3) does show chart recordings of hot-wire output for increasing Reynolds number Re = 50–90; and frequencies as a function of Reynolds number can be estimated from this. When that is done, one finds a

linear relationship between frequency and Reynolds number, which extrapolates to zero frequency for $Re = 0$ (to within the limitations of measuring frequencies from this figure). This linear relationship between frequency and Reynolds (or Rossby) number is characteristic of rod-induced waves, and not of type-II instabilities.

Tatro used a pair of non-disturbing hot-wire sensors to make phase measurements of the observed disturbances; and it was reported that the wave fronts of the type-II waves were aligned approximately parallel to the azimuthal direction. At first sight, this behaviour is not what is expected for the rod-induced waves. Their azimuthal perturbation velocity has no radial phase variations far from the disturbing rod. The waves propagate azimuthally; and wave fronts are aligned perpendicular to the azimuthal direction. The situation is different for measurements made near the disturbing rod, or more to the point, near the 'matched' layer where $V/r = m\omega$. A large phase shift in the radial direction ($\sim 180°$, see figure 11) occurs in this region and phase measurements can yield an apparent wave-front orientation parallel to the azimuthal direction. This apparent wave-front orientation will depend on wave structure, azimuthal wavenumber and the position of the sensors relative to the disturbing rod. A disturbing rod was used by Tatro to 'stimulate' the instability; but the relative position of the rod and sensors was not given. It is reasonable to assume proximity between sensors and rod, as the purpose of the rod was to increase the ambient turbulence level in the vicinity of the sensors. Such a situation could easily result in phase measurements interpreted as wave fronts aligned approximately parallel to the azimuthal direction.

A comparison between the data reported by Tatro and that obtained in the present study leads this author to conclude that the disturbances interpreted as type-II instabilities and inertial waves were rod-associated. The points of agreement between the two sets of data are as follows. (i) Frequencies were of the order of the rotation frequency; and this is lower than predicted for type-II waves. (ii) There is a linear relationship between frequency and Reynolds number (as estimated from Tatro, figure 3·3), which extrapolates to zero frequency for $Re = 0$. (iii) Disturbances were observed well outside the Ekman boundary layer. (iv) The critical Reynolds number against Rossby number data for different radii (see figures 14 (*a*), (*b*)) are more consistent with rod associated waves than type-II instabilities. The fact that Tatro observed no disturbances below $Re \simeq 55$, and the apparent alignment of wave fronts parallel to the azimuthal direction, can be explained in terms of rod-associated waves; the rest of Tatro's data cannot be reconciled with the characteristics of type-II instabilities.

Tatro & Mollo-Christensen reported observing a disturbance with properties similar to the type-I wave. It occurred at Re of approximately 125, and depended very weakly on Rossby number. The disturbance was confined to the boundary layer as measured with the non-disturbing probes. That is, the type I-wave was observed at sensors 3 mm from the wall, and not at sensors 6 mm from the boundary (Tatro 1966). From wave forms presented by Tatro, it appears that the type-I wave was subharmonically forced by the rod-associated wave. For

Re just less than the critical value for type-I waves, a 'high' frequency signal is shown; for Re just past critical for type-I waves, a wave of frequency one-half the previous value is present. The low-frequency mode is that confined to the boundary layer.

Caldwell & Van Atta reported observing a disturbance with properties similar to those predicted for the type-II instability. The frequencies were typically an order of magnitude greater than tbe rotation frequency; and data on vertical structure of the disturbance and frequency dependence on Reynolds number are all consistent with Ekman waves, and not rod-induced waves. The reason Caldwell & Van Atta were not plagued by rod-associated waves is believed to be related to the size of the annulus used. Tatro used a small annulus (R_0 = 45·7 cm) and a typical observation radius was around 30 cm. Caldwell & Van Atta used a large one (R_0 = 200 cm), and a typical observation radius was about 90 cm. For r_R = 90 cm, there is sufficient distance for the wake to decay fully downstream of the probe support. With the wake decayed, no restoring force exists, and rod waves cannot propagate 360° around the tank to reinforce themselves.

To complete the comparison with previous experiments, the attempt to observe Ekman instabilities will be discussed. Hot-wire sensors were placed at r = 0·333 and 0·500 and were 2 mm from the boundary. The rotation rate was Ω = 4·30 rad s^{-1} (δ = 1·89 mm), and the flux was varied up to approximately 3400 c^3 s^{-1}. This resulted in a maximum local Reynolds number of approximately 170 and 115 at r = 0·333 and 0·500, respectively. The anemometer outputs were observed using band-pass filters, and were also recorded and subsequently spectrum analysed. For both techniques, *no* signals were observed that could be interpreted as Ekman-layer instabilities. Spectral analysis showed a peak at the rotation frequency which represented system noise and amounted to less than 0·1 % of the ambient velocity. Spectral peaks at frequencies greater than Ω were also observed with amplitudes an order of magnitude smaller than the 'Ω' peak. The amplitude and frequency of these peaks were independent of local Reynolds number, and were also interpreted as system noise. Sources of this noise were believed to be associated with the rollers in the bearings and vibrations of the frame that supported the annulus.

The failure to observe Ekman instabilities in the present work does not contradict previous numerical and laboratory experiments. The type-I disturbances are either stationary or slowly moving, and if they were stationary, fixed sensors would not detect them. The type-II waves are rapidly moving disturbances with small growth rates. Using the theoretical results obtained by either Lilly or Faller & Kaylor (1966*b*), one can show that disturbances which begin to grow at large radii will have amplified a small amount (typically less than e^{+1}) by the time they reach the sensors at small radii. If the ambient turbulence level is very low, disturbances will not grow to detectable levels.

The ambient turbulence levels in the present experiment were believed to have been very low because of the very uniform inlet conditions at the source region. The source consisted of reticulated polyurethane foam approximately 8 cm thick with pores uniformly spaced at 20 cm^{-1}. No wave motions were

observed near the source for fluxes less than approximately 4000 $c^3\ s^{-1}$; and mean azimuthal velocity measurements, for fluxes less than about 2200 $c^3\ s^{-1}$, agreed well with theoretical predictions. These data support the conclusion that no unstable waves associated with the source region were present.

The very uniform and 'quiet' inlet conditions of the present experiment must be compared with the inlet conditions in the experiments of Faller and Caldwell & Van Atta. In Faller's experiment the incoming fluid entered through a thin slit (2 cm), and one can expect jetting of the fluid and higher turbulence levels than in the present experiment. The precise design of the source region for the annulus used by Caldwell & Van Atta is unclear; but in their experiments wave motions near the source were observed. These were believed to be centrifugal instabilities; and similar disturbances could be produced with the present apparatus under appropriate conditions. (For $\Omega = 4{\cdot}30$ rad s^{-1}, $S > 4000\ c^3\ s^{-1}$ would give rise to disturbances near the source.) These instabilities would certainly result in higher ambient turbulence levels than in the present experiment, where no such instabilities were present.

The theoretical work on Ekman-layer stability by Lilly and Faller & Kaylor (1966*b*) has been qualitatively verified by the laboratory experiments of Faller, Faller & Kaylor (1966*a*) and Caldwell & Van Atta. A rigorous quantitative verification of the theory remains to be carried out, and would require an apparatus with very low ambient turbulence levels. The disturbances could be selectively excited, as done by Schubauer & Skramstad (1948), to confirm the theory of Tollmien–Schlichting waves. The author regrets that time did not allow such a programme to be carried out, although curvature effects due to the annulus size would have complicated any results obtained with the present apparatus.

8. Conclusion

It has been demonstrated that hot-wire probe supports can give rise to azimuthally propagating disturbances in rotating annulus experiments. The disturbances are associated with the wake downstream of the probe support or disturbing rod. This wake decays with increasing distance from the rod, and gives rise to a non-azimuthally symmetric situation. Despite that lack of symmetry, the disturbances possess integer azimuthal wavenumbers, which range from $m = 2$ to 7, depending on the position of the disturbing rod. An inviscid model for an azimuthally symmetric wake in cylindrical geometry has a number of features which agree with experiment when wake parameters representative of the wake in the slowly decaying region (~ 40–80 cm downstream from rod) are used in the model.

Data presented on the onset of the disturbances are qualitatively consistent with the assumption that a circulation deficit, or wake, must extend around the annulus for the disturbances to propagate, although no quantitative relationship was found. The onset data show that decreasing the probe-support size increases the critical Rossby number for initiating disturbances; but disturbances can still arise for probes of the smallest practical size (~ 1 mm

diameter) in the present experiment. The data do indicate that a large annulus (observation radius ~ 100 cm), with small probe supports, will eliminate these disturbances, since there will be sufficient distance for the circulation deficit to decay.

These disturbances can be particularly troublesome in small annulus (annulus radius ~ 60 cm) experiments as they can occur near system parameters where other types of instabilities (such as Ekman-layer instabilities) occur. Comparison of present results with those of Tatro & Mollo-Christensen (1967) supports the conclusion that the wave motions interpreted as type-II Ekman instabilities and inertial eigenmodes were actually probe-associated disturbances. The same conclusion is reached about the wave motions believed to be inertial modes by Tatro (1966), Green (1968) and Ingram (1971). Therefore, at present, there is no laboratory evidence for the existence of a mechanism whereby Ekman-layer instabilities resonate with inertial eigenmodes, although Kaylor & Faller (1972) showed that a similar mechanism exists for internal waves in numerical experiments. The data on boundary-layer waves presented by Caldwell & Van Atta (1970) do not have characteristics similar to probe-associated disturbances; and it appears that true Ekman-layer instabilities were observed.

The author is indebted to Dr Richard L. Peskin of the Geophysical Fluid Dynamics Program at Rutgers University for his support and encouragement during this work, and his help in preparing the manuscript. The author wishes to thank Dr Isidoro Orlanski of the Geophysical Fluid Dynamics Laboratory at Princeton for his suggestions, which helped clarify this paper, and Mrs Gloria Calloway for typing the manuscript. Encouragement and many discussions with Dr E. Mollo-Christensen of the Massachusetts Institute of Technology, and Dr A. Green of the University of Michigan, are gratefully acknowledged. Research supported, in part, by the Atmospheric Sciences Section, National Science Foundation, NSF grant GA-33421.

REFERENCES

Barcilon, V. 1965 Stability of a non-divergent Ekman layer. *Tellus*, **17**, 53–68.

Bennetts, D. A. & Hocking, L. M. 1973 On nonlinear Ekman and Stewartson layers in a rotating fluid. *Proc. Roy. Soc.* A **333**, 469–489.

Betchov, R. & Criminale, W. O. 1967 *Stability of Parallel Flows*. Academic.

Burgers, J. M. 1953 Some considerations on turbulent flow with shear. *Proc. Netherlands Acad. Sci.* B **56**, 125–147.

Busse, F. 1968 Shear flow instabilities in rotating systems. *J. Fluid Mech.* **33**, 577–589.

Caldwell, D. & Van Atta, C. 1970 Characteristics of Ekman boundary-layer instabilities. *J. Fluid Mech.* **44**, 79–95.

Cerasoli, C. P. 1974 Experiments with a rotating source–sink annulus. Ph.D. thesis, Rutgers University.

Faller, A. J. 1963 An experimental study of the instability of the laminar Ekman layer. *J. Fluid Mech.* **15**, 560–576.

Faller, A. J. & Kaylor, R. E. 1966*a* Investigations of stability and transition in rotating boundary layers. *Dynamics of Fluids and Plasmas*. Academic.

FALLER, A. J. & KAYLOR, R. E. 1966*b* A numerical study of the laminar Ekman boundary layer. *J. Atmos. Sci.* **23**, 466–480.

FOX, L. 1959 *Boundary Problems in Differential Equations.* University of Wisconsin Press.

FULTZ, D. & KAISER, J. 1971 The disturbing effects of probes in meteorological fluid-model experiments. *J. Atmos. Sci.* **28**, 1153–1164.

GREEN, A. 1968 An experimental study of the interactions between Ekman layers and an annular vortex. Ph.D. thesis, Massachusetts Institute of Technology.

GREEN, A. & MOLLO-CHRISTENSEN, E. 1970 Laboratory observations of Ekman layer flow. *Dept. of Meteorology, Massachusetts Institute of Technology, Rep.* no. 70–4.

HIDE, R. 1968 On source–sink flows in a rotating fluid. *J. Fluid Mech.* **32**, 737–764.

HIDE, R. & TITMAN, C. W. 1967 Detached shear layers in rotating fluid. *J. Fluid Mech.* **29**, 39–60.

INGRAM, G. R. 1971 Experiments in a rotating source–sink annulus. Ph.D. thesis, Massachusetts Institute of Technology.

KAYLOR, R. E. & FALLER, A. J. 1972 Instability of the stratified Ekman boundary layer and the generation of internal waves. *J. Atmos. Sci.* **29**, 497–509.

LILLY, D. K. 1966 On the stability of the Ekman boundary flow. *J. Atmos. Sci.* **23**, 481–494.

SCHUBAUER, G. & SKRAMSTAD, H. 1948 Laminar boundary layer oscillations and stability of laminar flow. *N.A.C.A. Tech. Rep.* no. 909.

TATRO, P. R. 1966 Experiments of Ekman-layer instability. Ph.D. thesis. Massachusetts Institute of Technology.

TATRO, P. R. & MOLLO-CHRISTENSEN, E. 1967 Experiments on Ekman-layer instability. *J. Fluid Mech.* **28**, 531–44.